

# Generation of interfacial large amplitude waves at topography in three dimensions. New computations.

John Grue

Mechanics Division, Department of Mathematics  
University of Oslo, Norway  
e-mail: johng at math.uio.no

Trains of internal waves driven by tidal motion flow over topography typically show strong three-dimensionality, as exemplified in the internal wave generation in the Strait of Gibraltar, where wave crests propagate into the Mediterranean Sea, and at the Kara Gates in the High North, where the motion exhibits a fan propagating into the Barents Sea (see illustration). The wave generation is typically characterized by a strong effect of dispersion. Besides this, the nonlinearity is strong where the wave amplitude has a magnitude comparable to the depth of the pycnocline. The latter separates an upper layer with depth that is usually small compared to the total water depth. In some cases, the lower layer is thin and the upper layer deep. The wave motion is similar in the two cases.

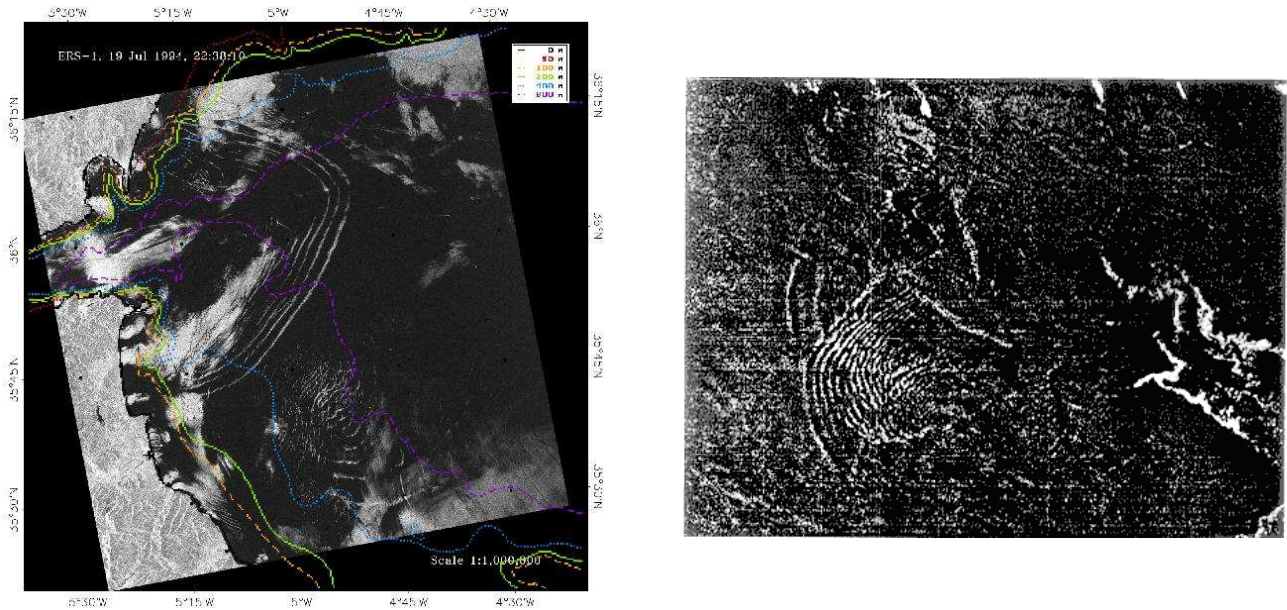


Figure 1: Three dimensional internal wave trains in Strait of Gibraltar (left) and Kara Gates (right) observed from satellite.

We study mathematically internal gravity waves moving along a thin pycnocline in a two-layer fluid with two homogeneous layers, including the effect of a variable topography. The effect of the tide is mimicked by moving the topography.

Potential theory with  $(\rho_1, h_1, \phi_1)$  (density, depth at rest, velocity potential) in the lower layer and similarly,  $(\rho_2, h_2, \phi_2)$  in the upper layer is employed. Horizontal coordinate  $\mathbf{x} = (x_1, x_2)$  and vertical coordinate  $y$  are introduced where  $y = 0$  separates the layers at rest. We shall assume that the rigid wall condition applies at the free surface, i.e. at  $y = h_2$ . The bottom topography is given by  $y = -h_1 + \beta(\mathbf{x}, t)$ .

The motion of a non-overtaking interface  $I$  at  $y = \eta$  is considered. Potentials evaluated at the interface are introduced by  $\phi_{I1}(\mathbf{x}, t) = \phi_1(\mathbf{x}, y = \eta, t)$  and  $\phi_{I2}(\mathbf{x}, t) = \phi_2(\mathbf{x}, y = \eta, t)$ . The kinematic and dynamic boundary conditions at the interface gives

$$\eta_t - V = 0, \quad (\phi_{I1} - (\rho_2/\rho_1)\phi_{I2})_t + (1 - \rho_2/\rho_1)g\eta + n.l.t.1 = 0, \quad (1)$$

where  $n.l.t.1 = \frac{1}{2} \left( |\nabla_1 \phi_{I1}|^2 - (\rho_2/\rho_1) |\nabla_1 \phi_{I2}|^2 - (1 - \rho_2/\rho_1)V^2 - 2V \nabla_1 \eta \cdot \nabla_1 (\phi_{I1} - (\rho_2/\rho_1)\phi_{I2}) + |\nabla_1 \eta \times \nabla_1 \phi_{I1}|^2 - (\rho_2/\rho_1) |\nabla_1 \eta \times \nabla_1 \phi_{I2}|^2 \right) / (1 + |\nabla_1 \eta|^2)$ ,  $\nabla_1 = (\partial_{x_1}, \partial_{x_2})$  denotes the horizontal gradient and

$V = \phi_{1n} \sqrt{1 + |\nabla_1 \eta|^2}$  a scaled normal velocity of the interface. An index  $n$  means the normal along the interface pointing into the upper fluid.

**Solution of the Laplace equation in the layers.** The prognostic equations (1) may be integrated once relations between  $(\phi_{I1} + \phi_{I2}, V)$  and  $(\phi_{I1} - (\rho_2/\rho_1)\phi_{I2}, \eta)$  are obtained. Solutions of the Laplacian potentials at the moving interface and at the variable sea bottom, for the lower potential, are obtained by using Green's theorem. The lower layer is bounded above by the interface  $I$  and below by the bottom topography  $B$ . The normal velocity at the interface and the velocity potential at the sea floor are obtained by the solution of a coupled set of integral equations. These are derived from the solution of the Laplace equation. For an evaluation point that is on the interface we obtain

$$\int_{I+B} \left( \frac{1}{r} + \frac{1}{r_1} \right) \frac{\partial \phi'_1}{\partial n'} dS' = 2\pi\phi_1 + \int_{I+B} \phi'_1 \frac{\partial}{\partial n'} \left( \frac{1}{r} + \frac{1}{r_1} \right) dS', \quad (2)$$

where  $r^2 = R^2 + (y' - y)^2$ ,  $r_1^2 = R^2 + (y' + y + 2h_1)^2$ ,  $\mathbf{R} = \mathbf{x}' - \mathbf{x}$ ,  $R = |\mathbf{R}|$ . In (2),  $\phi_1 = \phi_{I1}$  at  $I$ , and  $\phi_1 = \phi_{B1}$  at  $B$ . A similar equation is valid when the field point is located at the bottom. A similar equation is also valid in the upper layer, with the horizontal boundary at  $y = h_2$ .

The difficulty is to accurately obtain the normal velocities at the interface. Here the method of successive approximations is used for this purpose. For the normal velocity in the lower and upper layers we obtain

$$V = \phi_{1n} \sqrt{1 + |\nabla_1 \eta|^2} = V^{(1)} + V^{(2)} + V^{(3)} + \dots, \quad W = \phi_{2n} \sqrt{1 + |\nabla_1 \eta|^2} = W^{(1)} + W^{(2)} + W^{(3)} + \dots \quad (3)$$

A central point is that these expansions converge very rapidly. In the computations we include two or three terms in the expansions, where the magnitude of the remaining terms are used to illustrate the usefulness of the method. Reference computations illustrate that these are very small. In practice there is no difference in the computations using two and three terms, even for wave amplitude comparable to the thinner layer (order one). Numerical computations illustrate the curved wave generation at geometry (Fig. 2).

The method may also be used to compute the waves and wave resistance in the dead-water problem, first explained by Fridtjof Nansen on his ship FRAM, during the Polar Expedition (1893-96). We illustrate the importance of the nonlinear terms on the internal wave resistance, previously computed by linear theories only. New, nonlinear computations show that the wave resistance becomes 100 times larger in strong dead water!

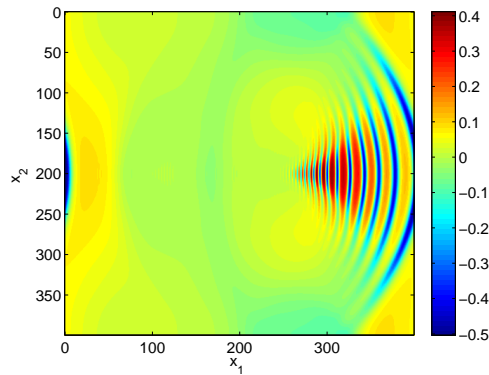


Figure 2: Numerical computation of curved internal waves of large amplitude, driven by tide over topography.